Journal of Power Sources 260 (2014) 12–18

Contents lists available at ScienceDirect

Journal of Power Sources

journal homepage: www.elsevier.com/locate/jpowsour

Effect of stabilizers on the synthesis of palladium–nickel nanoparticles supported on carbon for ethanol oxidation in alkaline medium

Huijuan Yang [a], Hui Wang [a], Hao Li [b], Shan Ji [c,1], Moegamat Wafeeq Davids [c], Rongfang Wang [a,*]

[a] Key Laboratory of Eco-Environment-Related Polymer Materials of Ministry of Education of China, College of Chemistry and Chemical Engineering, Northwest Normal University, Lanzhou 730070, China
[b] Department of Chemical Engineering, Huizhou University, Huizhou, Guangdong 516007, China
[c] South African Institute for Advanced Materials Chemistry, University of the Western Cape, Private Bag X17, Bellville, Cape Town 7535, South Africa

HIGHLIGHTS

- PdNi/C catalysts were prepared by the different stablizers such as glycine.
- The stablizers influence not only the distribution but also the alloy degree of PdNi/C.
- The catalytic activities of PdNi/C catalysts are related to the lattice contraction.

ARTICLE INFO

Article history:
Received 21 December 2013
Received in revised form
23 February 2014
Accepted 28 February 2014
Available online 12 March 2014

Keywords:
Palladium–nickel nanoparticle
Different stabilizers
Electrocatalyst
Ethanol oxidation

ABSTRACT

PdNi/C electrocatalysts for ethanol oxidation in alkaline medium are fabricated using four stabilizers, i.e., glycine (G), ethylene diamine tetraacetic acid (EDTA), sodium citrate (SC), and sodium dodecyl sulfate (SDS) with the same reducing process and reaction parameters. X-ray diffraction characterization shows PdNi nanoparticles for all PdNi/C electrocatalysts possess face-centered cubic structure with different alloying degree. TEM results show that PdNi/C-G and PdNi/C-SC have uniform dispersion with ellipse morphology, while particle agglomeration occurs on PdNi/C-EDTA and PdNi/C-SDS. Electrocatalytic activities of these PdNi/C electrocatalysts for ethanol oxidation are measured by cyclic voltammetry and chronoamperometry techniques. The electrocatalytic activities of PdNi/C change with the different lattice contraction. PdNi/C-SC electrocatalyst exhibits the best activity among the four electrocatalysts, which is ascribed to an appropriate lattice contraction.

1. Introduction

Direct ethanol fuel cells (DEFCs) based on ethanol fuel have received a growing interest in recent years as strong candidates for portable power sources, electric vehicles and transportation applications owing to a high energy density of ethanol (~8 kW h kg^{-1}), less toxicity and ease in handling and transportation [1,2]. In addition, ethanol is a sustainable fuel, which can be produced in large quantities through the fermentation of sugar-containing raw materials. On the anode electrode, ethanol molecules are completely oxidized into CO_2 involving the release of 12 electrons and the cleavage of the C–C bond [3]. However, electron affinity or ionization energy between the two C atoms of the C–C bond is little, which make it difficult to activate the C–C bond breaking, particularly, in acid medium [4]. Therefore, designing and developing efficient anode electrocatalysts for DEFCs in alkaline medium has become a hot topic in research.

Pd has been proved to be a promising electrocatalyst for ethanol oxidation in alkaline medium, showing higher activity than Pt [5]. Beside, it is at least fifty times abundant on earth than Pt. However, the catalytic activity of Pd for ethanol oxidation in alkaline medium needs to be enhanced [6]. Many efforts have been contributed to

* Corresponding author. Tel./fax: +86 931 7971533.
E-mail addresses: sji@uwc.ac.za (S. Ji), wrf38745779@126.com, wangrf@nwnu.edu.cn (R. Wang).
[1] Tel.: +27 21 9599316.

http://dx.doi.org/10.1016/j.jpowsour.2014.02.110
0378-7753/

further improvement of the catalytic activity of Pd. One approach is to seek a support with large surface areas, such as graphene [7], carbon nanofibers [8], carbon nanotube [9], porous carbon spheres [10], TiN [11]. Another trend is alloying Pd with other metals, for instance, Pt [12], Au [13], Ag [14], Sn [15], Co [16,17], Ni [17,18], or combining Pd with metal oxides (for example, SnO_2 [19], In_2O_3 [20]). Among the various developed binary Pd composite, the binary PdNi electrocatalysts are regarded as the most attractive catalysts in alkaline medium [8,16,17].

Till now, there are a variety of methods for preparing PdNi electrocatalysts for ethanol oxidation in alkaline medium [21–24], the simultaneously chemical reduction reaction is widely used. However, the optimum ratio of Pd:Ni for PdNi electrocatalysts is varied in these reports. For example, Shen et al. [25] reported that Pd_2Ni_3/C as a promising candidate for ethanol oxidation compared to other Pd_xNi_y/C catalysts. Zhang et al. [22] described the optimized Pd_4Ni_5/C as a promising anode catalyst for alkaline DEFCs by giving more negative EOR onset potential and the higher exchange current density than other Pd_xNi_y/C. Besides the examples, there were other different results also reported [23,26]. These different results were caused by the different stabilizing agents and reductants, which influence the formation of particle nucleation and growth of nanoparticles as well as the composition of the nanoparticles. Thus, a systematic study on the stabilizer-mediated synthesis of PdNi catalysts and their electrocatalytic for ethanol oxidation in alkaline medium using various types of stabilizers and reductants is necessary.

In our previous work, the effect of the stabilizers on the synthesis of Pt/PdSn–SnO_2/C [27] and PtSn/C [28] catalysts for ethanol oxidation has been studied. We found that the stabilizers not only involve the formation of alloy structure but also control the morphologies of nanoparticles such as size, size distribution, and dispersion. To the best of our knowledge, the preparation of binary PdNi electrocatalysts on carbon by the simultaneously chemical reduction reaction using different stabilizers has been rarely reported. Based on the above literature and our previous work, the effects of various stabilizers on the synthesis and activity of PdNi/C electrocatalyst for ethanol oxidation in alkaline medium were systematically investigated in this study. We have used four different types of stabilizers, such as glycine (G), sodium citrate (SC), ethylene diamine tetraacetic acid (EDTA), and sodium dodecyl sulfate (SDS). PdNi/C electrocatalysts have been synthesized by the chemical reduction method in the presence of these stabilizers using $NaBH_4$ as the reductant. The synthesized PdNi/C catalysts were analyzed by various spectroscopic and electrochemical methods to define the correlation between the stabilizers and the properties of synthesized catalysts.

2. Experimental

2.1. Preparation of PdNi/C electrocatalysts

PdNi/C electrocatalysts were prepared by $NaBH_4$ reduction method, which was carried out in ultra pure water. PdNi/C electrocatalysts with Pd:Ni atomic ratio of 1:1.12 were prepared as follows: 20.8 mg of $PdCl_2$ and 25.3 mg of $NiCl_2 \cdot 6H_2O$ were dissolved in 30 mL ultra water in a 100 mL flask. Then the stabilizer, i.e., 260 mg of G, was added and kept stirring for 0.5 h. Pretreated carbon black Vulcan XC-72 (50 mg) was added to the mixture with stirring. After that, 20 mL of 0.1 mol L^{-1} $NaBH_4$ aqueous solution was added slowly to the mixture and kept stirring for 3 h. The resultant, PdNi-G/C, was collected by filtrating, washed with ethanol and deionized water, and dried in air at 60 °C for 12 h.

Subsequently, EDTA, SC, and SDS were used to prepare PdNi/C electrocatalysts. Taking into account the effect of the concentration of the stabilizers on morphology and disperse of metal particles, the normal molar ratio of the stabilizer and metal ion ($Pd^{2+} + Ni^{2+}$) is ca. 1:2 for G, EDTA and SC, and ca. 1:4 for SDS. It should be noted that the quantities of these stabilizers are light excess. The procedures were the same as the above one, except 100 mg of SC, 100 mg of EDTA and 190 mg of SDS were added as stabilizer instead of G, respectively.

2.2. Characterization

X-ray diffraction (XRD) patterns of the catalysts were recorded on a Shimadzu XD-3A diffractometer (Japan) using filtered Cu Ka radiation. Transmission electron microscopy (TEM) measurement was carried out on a JEM-2010 Electron Microscope (Japan) with the acceleration voltage of 200 kV. The average chemical compositions of the catalysts were determined using an IRIS advantage inductively coupled plasma atomic emission spectroscopy (ICP-AES) system (Thermo, USA).

2.3. The electrochemical measurements

The electrochemical measurements were performed using an CHI600D electrochemical workstation ([H] CH Instruments, Inc). A common three-electrode electrochemical cell system was used for the measurements. The counter and reference electrodes were a platinum wire and an Hg/HgO (1 mol L^{-1} KOH 0.967 V *vs.* RHE) electrode, respectively. The working electrode was a glassy carbon disk (5 mm in diameter). The thin-film electrode was prepared as follows: 5 mg of catalyst were dispersed ultrasonically in 1 mL Nafion/ethanol (0.25% Nafion) for 15 min. 8 μL of the dispersion was transferred onto the glassy carbon disk using a pipette, and then dried in the air. All the electrochemical experiments were conducted at ambient temperature. For CO-stripping tests, CO was first adsorbed on the working electrode by bubbling CO through the cell for 5 min; the working electrode was then transferred to another cell containing nitrogen-saturated 1.0 mol L^{-1} KOH electrolyte for testing.

3. Results and discussion

Fig. 1 shows molecular structures of the four stabilizers used in the synthesis of PdNi/C electrocatalyst. The characteristics in the structure and chemical state, including i) the length of the alkyl chain and configuration, ii) non-ionic *vs.* ionic nature, and iii) the atoms which would be in coordination with the metal ions, are different among the four stabilizers. In the process of the formation of binary PdNi nanoparticles, the reaction to form metal complex between metal ions and the stabilizers is the primary step. At the same time, a competitive reaction between the metal precursors and the reductant occurs simultaneously. The rates of these two reactions influence the formation of PdNi particle nucleation and growth of nanoparticles as well as the composition of the PdNi nanoparticles. Thus, the different characteristics of these four stabilizers would cause different impact on the structure and composition which would lead to the different electrochemical performance of PdNi/C electrocatalysts.

Bulk structural information of the PdNi/C electrocatalysts prepared under different stabilizers was obtained by XRD and is shown as Fig. 2. For comparison, XRD pattern of home-made Pd/C [29] is also shown as the vertical line in Fig. 2. It can be seen that there are five diffraction peaks for the all electrocatalysts. The first peak centered at $2\theta = 24.8°$ is assigned to the graphite (002) facet of the Vulcan carbon [30], and the other four peaks located at the 2θ values of ca. 40, 47, 68, and 82° are related to the (1 1 1), (2 0 0), (2 2 0) and (3 1 1) facets of the face-centered cubic (fcc) crystalline Pd

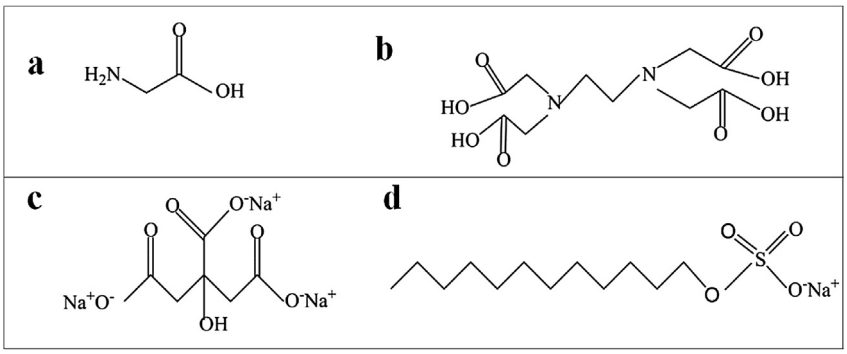

Fig. 1. Molecular structures of the stabilizers used in the synthesis of PdNi/C electrocatalysts; (a) G, (b) EDTA, (c) SC, and (d) SDS.

[29], respectively. For the series of the PdNi/C electrocatalysts, there are no visible peaks attributed to the characteristic peak of Ni oxide. However, the presence of Ni oxides in the form of amorphous oxides cannot be discarded. The mean crystallite sizes are estimated using Scherrer's equation (1) [31]:

$$d = \frac{0.90\lambda}{\beta_{2\theta}\cos\theta} \quad (1)$$

where d is the grain diameter, λ is X-ray radiation wavelength, $\beta_{2\theta}$ is the width of half peak, and θ is the diffraction angle. The mean crystallite sizes estimated from the Pd (1 1 1) diffraction peaks listed in Table 1 are 6.3, 5.7, 5.4 and 6.5 nm for PdNi/C-G, PdNi/C-EDTA, PdNi/C-SC, and PdNi/C-SDS, respectively. It indicates that the different stabilizers have an effect on the mean crystallite size.

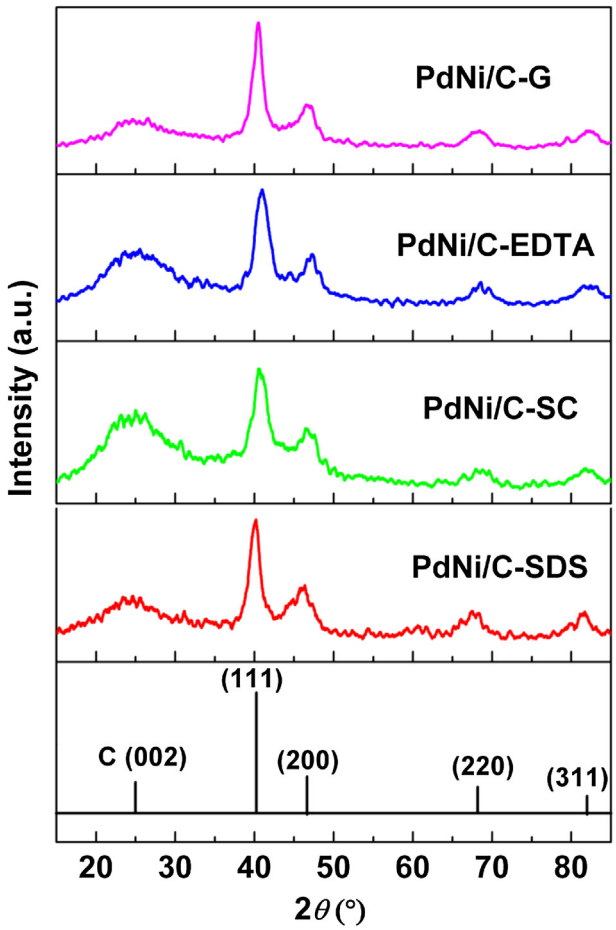

Fig. 2. XRD patterns of all PdNi/C electrocatalysts, and XRD pattern of Pd/C shown as the vertical line.

In the work of Zhang et al. [22], Ni is hard to alloy well with Pd using $LiBet_3H$ as the reductant. The weak-alloying of Pd and Ni in PdNi/C electrocatalysts, which synthesized by simultaneous reduction method using $NaBH_4$ as the reductant, was also reported by Shen et al. [25]. In our work, by comparison with the characteristic peaks of Pd/C, no peak shift is observed for PdNi/C-SDS electrocatalysts, indicating Ni atoms are un-alloyed with Pd atoms; and a small shift is observed for PdNi/C-G electrocatalysts, suggesting a little Ni atoms are alloyed with Pd atoms. However, the diffraction peaks of PdNi/C-EDTA and PdNi/C-SC electrocatalysts has obviously positive shifts, suggesting the formation of PdNi alloy. Based on the literature and our work, the stabilizers could influence the alloying degree of binary PdNi nanoparticles. Similar work has been extensively studied for other binary metal nanoparticles, such as PtSn and PtCo nanoparticles [32,33]. Furthermore, the shift of the Pd (111) peak follows the order PdNi/C-EDTA > PdNi/C-SC > PdNi/C-G > PdNi/C-SDS ≈ Pd/C.

Here, we try to elucidate roughly the correlation between the alloy degree and the different stablizers. In the process of preparing PdNi nanoparticles, coordination compounds between metal ions and the stabilizers is firstly formed. The donor atoms are N and O atoms for G and EDTA, O atom for SC and SDS, and the number of the donor atoms is two, six, four and four for G, EDTA, SC, and SDS, respectively. The chelate compound between the metal ion (Pd^{2+} and Ni^{2+}) and the ligands (G, EDTA and SC), is formed. The chelate compound between the metal ion and SDS cannot be formed because the stable chelate ring, five-membered ring or six-membered ring, cannot be formed. While, for EDTA and SC, multiple chelate rings are formed. Moreover, the number of chelate rings for EDTA is five, more than that of SC, leading to that the chelate compound of EDTA is stable than that of SC due to chelate effect. It can be inferred that the stability of the coordination compounds is in the order of EDTA > SC > G > SDS.

Table 1
Structural parameters of the PdNi/C electrocatalysts.

Catalyst	PdNi/C-G	PdNi/C-EDTA	PdNi/C-SC	PdNi/C-SDS
The mean crystallite size/nm	6.3	5.7	5.4	6.5
Lattice constant/Å	3.8990	3.8902	3.8935	3.9080
The loading of metal/wt%	22.8	21.9	22.2	23.0
Pd:Ni atom ratio	1:1.10	1:1.12	1:1.10	1:1.11
The average particle size/nm	6.5	7.7	10.6	–

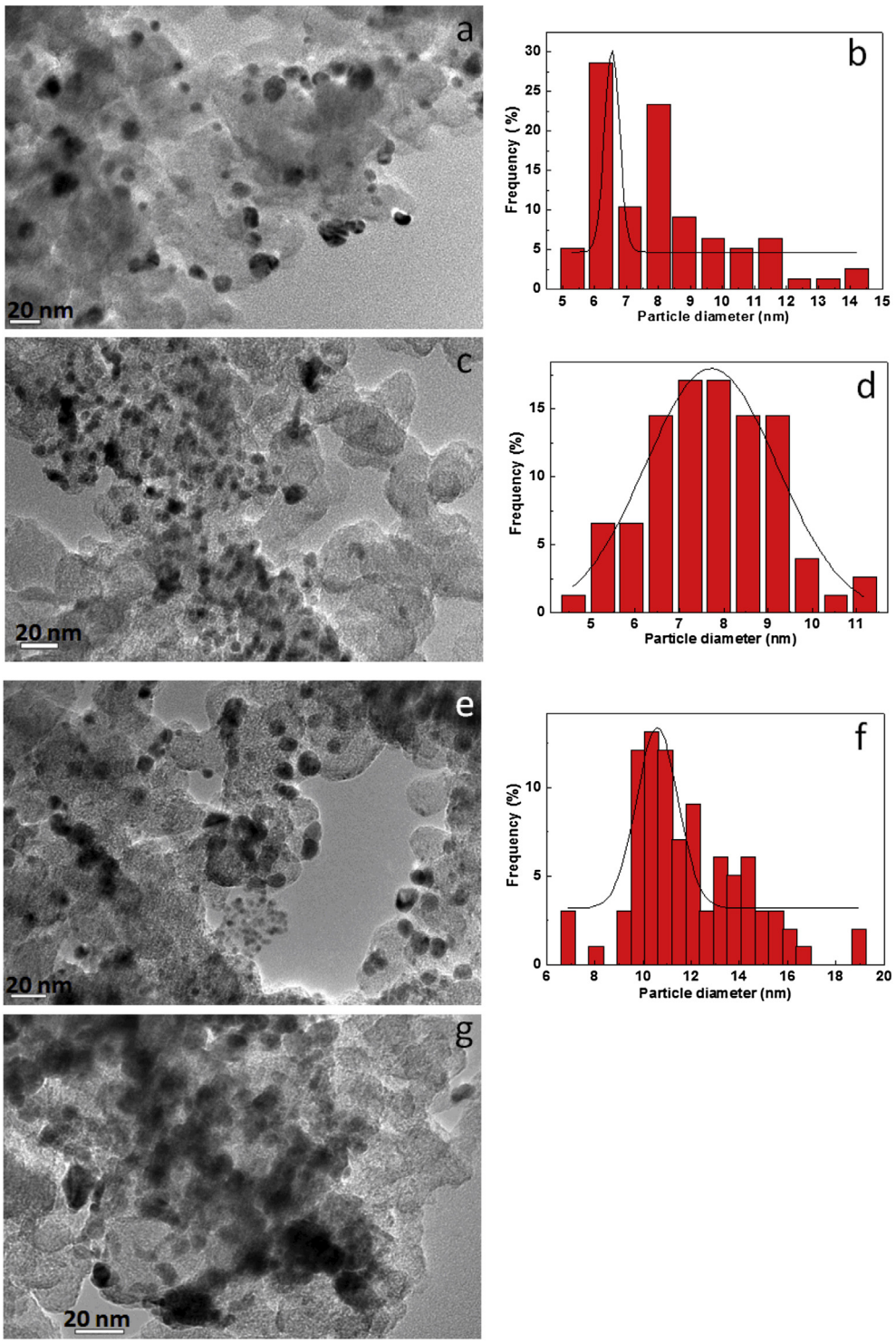

Fig. 3. Representative TEM images and the corresponding particle size distribution histograms of (a and b) PdNi/C-G, (c and d) PdNi/C-EDTA, (e and f) PdNi/C-SC, and (g) PdNi/C-SDS.

When the reductant, $NaBH_4$, is added, a reduction reaction between the metal precursors and the reductant occurs. The two reactions are competitive. More stable the complexes are, the slower the rate of the reduction reaction. Thus, the rate of the reduction reactions from SDS, G, SC to EDTA decreases. We believe that the slow reaction rate may provide more opportunity for Ni atoms to penetrate the lattice of Pd, which results in the high alloying degree.

The lattice parameters for the four catalysts are calculated according to Equation (2) [3,28]:

$$a_{(\mathrm{fcc})} = \frac{\sqrt{2}\lambda}{\sin\theta} \tag{2}$$

where $\alpha_{(\mathrm{fcc})}$ is the lattice parameter and λ is the X-ray radiation wavelength and θ is the diffraction angle. The obtained lattice

parameters for the four catalysts are tabulated in Table 1. It can be observed that the lattice parameter of PdNi/C-EDTA and PdNi/C-SC electrocatalysts is obviously decrease compared with that of Pd/C, revealing a lattice contraction due to the partial replacement of Pd sites in PdNi alloy by smaller Ni atoms [34].

Fig. 3 presents the TEM images of all PdNi/C electrocatalysts and their corresponding particle size distribution histogram. For the PdNi/C-G electrocatalyst shown in Fig. 3a, the PdNi nanoparticles has an ellipse shape and are evenly dispersed on the carbon surface. By counting the size of PdNi nanoparticles in Fig. 3a, the particle size distribution is obtained, which is displayed in Fig. 3b. The average diameter of the PdNi nanoparticles is ca. 6.5 nm, which is close to the XRD result. In the case of PdNi/C-EDTA (Fig. 3c), most elliptic PdNi nanoparticles are scattered on the surface of a few carbon particles, and the occurrence of agglomeration can be observed. The size of the PdNi nanoparticles in Fig. 3d ranges from 4.6 nm to 11.2 nm. The average diameter of the PdNi nanoparticles is ca. 7.7 nm, which is obviously larger than the XRD result due to the agglomeration. XRD gives information on the size of a coherent scattering domain, agglomerates, comprising crystallites with different lattice orientations, which appear in XRD patterns undistinguishable from isolated particles. Thus, the obvious difference of particle size obtained from XRD and TEM is inevitable. The particle agglomeration is often not considered in utilization of TEM rather than XRD for determining particle dispersion. Fig. 3e shows that the dispersion of PdNi/C-SC is uniform. The particle size of PdNi nanoparticles in Fig. 3f is in a broad range from 6.9 nm to 18.9 nm with 10.6 nm the average particle size. For PdNi/C-SDS electrocatalyst (Fig. 3g), most PdNi nanoparticles are concentrated onto the surface of a few carbon particles, and severe agglomeration occurs, consequently resulting in the particle size being difficult to estimate. As the previous discussion about XRD characterization, the reduction reaction in SDS system is faster than others; thus, the distribution of PdNi nanoparticles is very poor. Similarly, the particle distribution for EDTA, and SC is relatively better than that of G. TEM results clearly show that the distribution and size of PdNi nanoparticles are affected by the stabilizers.

The actual bulk compositions of all PdNi/C electrocatalysts, measured by ICP, are presented in this Table 1. The Pd:Ni atomic ratios are close to 1:1.1. The metal loading for each catalyst is similar, and slightly lower than that in the precursors.

The electrochemical properties of the four PdNi/C electrocatalysts were first detected by cyclic voltammetry technique. Fig. 4 shows the cyclic voltammograms (CVs) of the four PdNi/C electrocatalysts with various stabilizers. In the CVs of the four PdNi/C electrocatalysts, one can observe a broad peak in the lower potential region (from 0.277 to 0.567 V) on the forward scan, which can be assigned to the OH^- adsorption on the surface of PdNi/C electrocatalysts, following a peak at higher potential at ca. −0.16 V, corresponding to the water activation on Pd [21,22]. On the reverse sweep, the defined peak near −0.06 V is characteristic of the reduction of Pd oxide to Pd.

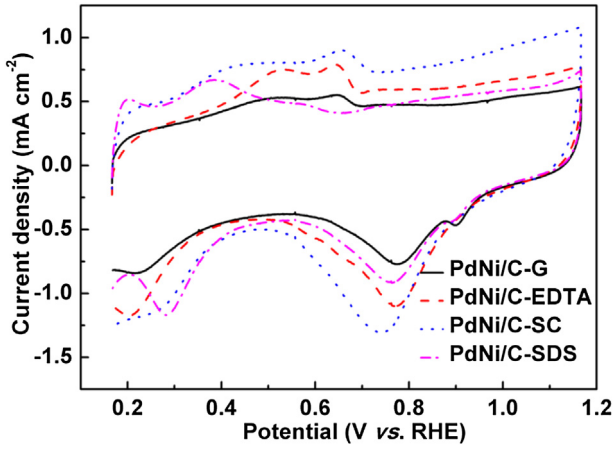

Fig. 4. Cyclic voltammograms of the four PdNi/C electrocatalysts in nitrogen-saturated 1.0 mol L^{-1} KOH solution at a scan rate of 50 mV s^{-1}.

Considering the penetration of hydrogen into the Pd and Pd-based bimetallic nanostructures, the electrochemical surface area (ECSA) of the all PdNi/C electrocatalysts are estimated by the charge of the reduction region of PdO to Pd, and are summarized in Table 2. It is found that PdNi/C-SC has the largest ECSA among the four catalysts, implying that it would exhibit higher catalytic activity for ethanol oxidation than others.

The electrocatalytic activities of all PdNi/C electrocatalysts for ethanol oxidation were characterized by cyclic voltammetry technique in the mixture of 1 mol L^{-1} KOH + 1 mol L^{-1} CH_3CH_2OH solution at a scan rate of 50 mV s^{-1}. The obtained results are plotted in Fig. 5. Ethanol oxidation is characterized by two well-defined oxidation peaks, designated as Peak I, located at ca. 0.887 V in the anodic sweep curve, and Peak II, centered at ca. 0.747 V in the cathodic sweep curve, respectively. The current density was normalized by the Pd loading on the electrode. The current density on PdNi/C-SC electrode is clearly larger than those on the other three PdNi/C electrodes in all potential regions. The current density of all PdNi/C catalysts at 0.567 V is summarized in Table 2. It can be concluded that the order of the current density for ethanol oxidation is PdNi/C-SC > PdNi/C-EDTA > PdNi/C-G > PdNi/C-SDS.

It is of interest to compare the onset potential of Peak I observed in this work with those supported PdNi electrocatalysts reported in the literature. Such a comparison is, however, complicated by their dependence on the experimental condition, such as temperature, sweep rate, and nature of supporting electrolyte. The onset potential of our catalysts along with the literature values for bimetallic PdNi catalysts are collected in Table 2. Because the reference electrode used in literature is different, the potential was referred to NHE by us for intuitively comparison. From Table 2, it can seen that the onset potential for ethanol oxidation on PdNi/C-SC electrode is lower than the values reported in Ref. [21,35,26], comparable to that in Ref. [25], and higher than that in Ref. [22]. Such a result indicates that it is not only the natural properties, including the

Table 2
Electrochemical performance of the as-prepared PdNi/C electrocatalysts and other PdNi electrocatalysts reported.

Electrocatalyst	ECSA ($m^2\ g^{-1}_{Pd}$)	The onset potential of peak I	The current density of at −0.26 V ($mA\ mg^{-1}_{Pd}$)
PdNi/C-G	14.5	0.354 V *vs.* RHE	155.8
PdNi/C-EDTA	30.7	0.342 V *vs.* RHE	180.6
PdNi/C-SC	38.2	0.314 V *vs.* RHE	321.3
PdNi/C-SDS	20.5	0.314 V *vs.* RHE	253.3
PdNi/MCNTs [21]	–	−0.60 V *vs.* SCE[a] (0.469 V *vs.* RHE)	–
Pd_2Ni_3/C [25]	–	−0.65 V *vs.* Hg/HgO[b] (0.317 V *vs.* RHE)	–
Pd_4Ni_5/C [22]	–	−0.801 V *vs.* Hg/HgO (0.066 V *vs.* RHE)	–
PdNi/SF-MWCNT [35]	–	−0.5 V *vs.* Ag/AgCl[c] (0.524 V *vs.* RHE)	–
$Pd_{59}Ni_{41}$/C [26]	–	−0.56 V *vs.* Ag/AgCl (0.464 V *vs.* RHE)	–

[a] Its potential is 0.242 V *vs.* NHE.
[b] Its potential is 0.140 V *vs.* NHE.
[c] Its potential is 0.197 V *vs.* NHE.

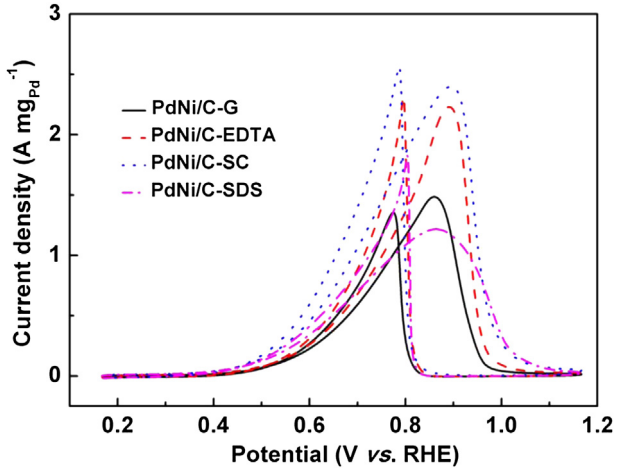

Fig. 5. Cyclic voltammograms of the four PdNi/C electrocatalysts in nitrogen-saturated 1.0 mol L^{-1} KOH + 1.0 mol L^{-1} CH_3CH_2OH solution at a scan rate of 50 mV s^{-1}.

Pd:Ni ratio, metal dispersion, and the support, which determined the catalytic activity in ethanol oxidation, but also the experimental conditions. It cannot be found the best bimetallic PdNi catalysts in the all catalysts listed in Table 2 due to the lack of the same test conditions.

On the other hand, it is worth to correlate the catalytic activity of PdNi/C electrocatalysts with its physical characterization in this work. As we know, the activity of binary or polymetallic electrocatalysts depends on several parameters, such as particle size distribution and morphology, alloying degree, bulk and surface composition. These factors can be controlled to enhance the activity of the catalysts by optimizing the synthesis parameters. Thus, the first factor, we considered, is particle size distribution and morphology. PdNi/C-SDS electrocatalyst shows severer agglomeration in Fig. 3g compared with other electrocatalysts, thus leading to the poor catalytic activity; While, PdNi/C-G electrocatalyst possess uniform distribution and the smallest average particle size among the four electrocatalysts, but does not exhibit higher catalytic activity than PdNi/C-EDTA and PdNi/C-SC electrocatalysts. The contradictory conclusions suggest that the main reason for the different catalytic activities amongst the four PdNi/C electrocatalysts cannot be associated with the variation of particle size distribution and morphology.

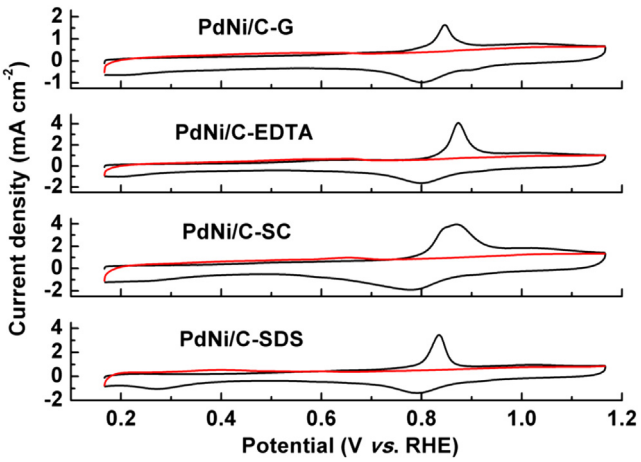

Fig. 6. CO-stripping voltammograms of the PdNi/C electrocatalysts in nitrogen-saturated 1.0 mol L^{-1} KOH solution at 50 mV s^{-1} of scan rate.

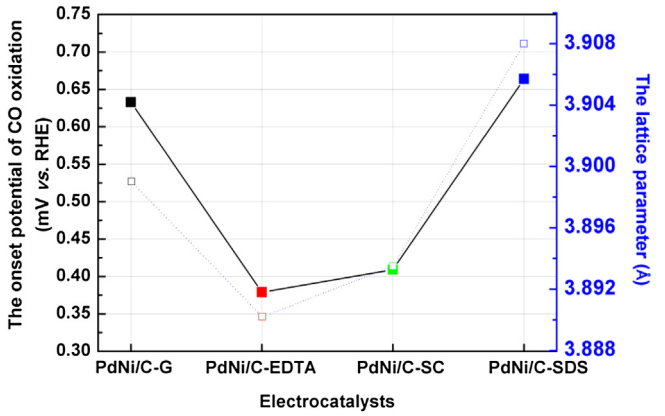

Fig. 7. The onset potential of CO oxidation on the PdNi/C electrodes and the trend of the lattice parameters of the four PdNi/C.

Another important factor influencing the catalytic activity is the structure of PdNi nanoparticles. The information provided by XRD indicates that binary PdNi nanoparticles of the four electrocatalysts have fcc structure, but the different lattice parameters due to the lattice contraction resulting from the different alloying degree. In our previous work [27,36,37] and other research [38,39], it is found that the lattice contraction in Pd-based systems squeezed Pd atoms, leading to the increased overlap of the d orbital, and consequently the band broadens. The adsorption of intermediate products from the oxidation of methanol or ethanol, such as CO, becomes difficult, thus changes the catalytic activity. Furthermore, the phenomenon can be confirmed by CO-stripping voltammetry test.

Here, based on the above discussion, a hypothesis which emerges from the analysis of the XRD result, we propose, is that the change of catalytic activity for PdNi/C electrocatalysts might be due to the stain effect. Then, CO-stripping test on PdNi/C electrodes was carried out in 1 mol L^{-1} KOH solution at a scan rate of 50 mV s^{-1} and presented in Fig. 6. It can be seen that the adsorbed CO has been oxidized completely in the first scan, and no CO oxidation is monitored during the second scan for all PdNi/C electrocatalysts. For PdNi/C-G and PdNi/C-SC electrocatalysts, a CO-oxidized peak appears. While, a splitting CO-oxidized peak is presented for PdNi/C-EDTA and PdNi/C-SDS, which may be ascribed to the agglomeration of PdNi nanoparticles. The CO-oxidized onset potential of the four electrocatalysts is plotted in Fig. 7. In order to correlate between the trend of the CO-oxidized onset potential and that of the lattice parameters, the trend of the lattice parameters are also plotted in Fig. 7. It clearly shows that the trend of the onset potential of CO oxidation is PdNi/C-EDTA < PdNi/C-SC < PdNi/C-G < PdNi/C-SDS, which is in accordance with the trend of the lattice parameters.

However, why does PdNi/C-SC show the highest catalytic activity among the four electrocatalysts, not PdNi/C-EDTA? Based on the previous study [22,40], the mechanism of ethanol oxidation reaction on PdNi/C electrode could be descried through the following process:

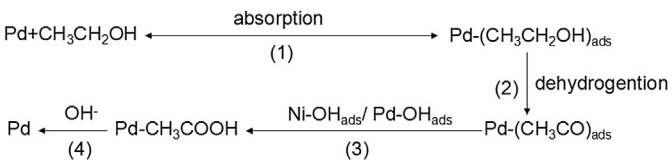

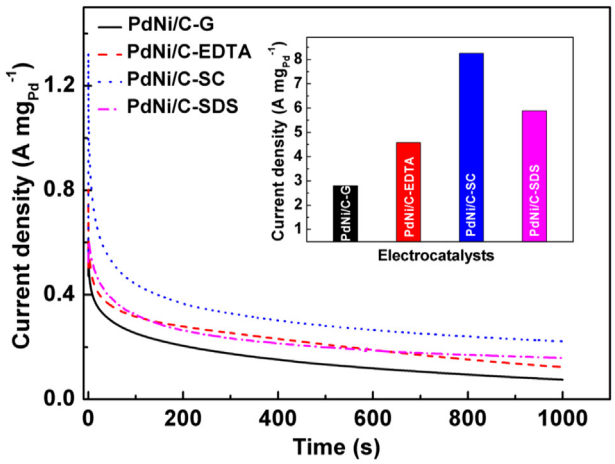

Fig. 8. Chronoamperometry tests for ethanol oxidation in 1.0 mol L^{-1} KOH + 1.0 mol L^{-1} CH_3CH_2OH on the four PdNi/C electrocatalysts at 0.467 V *vs.* RHE.

The smaller lattice contraction is the higher electron density of the *d*-band of Pd, which results in the decrease of the binding strength for reaction intermediates and the enhancement of step (3). However, the electron produced in the step (2), dehydrogenation reaction, would be difficultly accepted by Pd atoms with high electron density, causing that step (2) would be impeded. Hence, it is obvious that the optimal catalytic activity is obtained by well-balanced step (2) and (3) on the PdNi/C-SC electrode.

Fig. 8 shows the current density–time curves measured at a constant potential at 0.467 V. In the curves of the all PdNi/C electrocatalysts, the oxidation currents rapidly decrease from 0 to 100 s, likely due to the formation of intermediate and poisoning species, such as CO_{ads}, during the ethanol oxidation reaction. With time, a pseudo-steady state is achieved. After a polarization of 1000 s, the electrodes of PdNi/C-G, PdNi/C-SC, and PdNi/C-SDS reach their steady-state current density of 75.5, 123.3, 222.5 and 158.7 mA mg_{Pd}^{-1}, which are shown as the inset. It can be seen that the current density of ethanol oxidation on PdNi/C-SC electrode is higher than those on other PdNi/C electrodes, as found above in the CV tests; and the steady-state current density is in the order PdNi/C-SC > PdNi/C-EDTA > PdNi/C-SDS > PdNi/C-G. The facts indicate that as-prepared PdNi/C electrocatalysts with different stabilizers have different durability for poisoning species owing to the different lattice contraction.

4. Conclusions

Four types of stabilizers, G, EDTA, SC, and SDS, were used to prepare PdNi/C electrocatalysts, which resulted in different PdNi nanoparticles formed on the carbon support. Stabilizers have an obvious impact on the morphology, particle distribution, and the alloying degree of synthesized PdNi nanoparticles. The electrocatalytic activities towards ethanol oxidation of the four PdNi/C electrocatalysts decrease in the order: PdNi/C-SC > PdNi/C-EDTA > PdNi/C-G > PdNi/C-SDS. Variation of electrocatalytic activity is attributed to the different degree of the lattice contraction.

Acknowledgments

The authors would like to thank the National Natural Science Foundation of China (21363022, 21163018, and 51362027) for financially supporting this work.

References

[1] S. Nguyen, H. Law, H. Nguyen, N. Kristian, S. Wang, S. Chan, X. Wang, Appl. Catal. B 91 (2009) 507–515.
[2] X. Wang, H. Wang, Z. Lei, Z. Zhang, R. Wang, Chin. J. Catal. 32 (2011) 1519–1524.
[3] J. Cai, Y. Huang, Y. Guo, Electrochim. Acta 99 (2013) 22–29.
[4] J. Barroso, A. Pierna, T. Blanco, E. Morallón, F. Huerta, J. Power Sources 196 (2011) 4193–4199.
[5] Q. Yi, F. Niu, L. Sun, Fuel 90 (2011) 2617–2623.
[6] J. Yin, S. Shan, M. Ng, L. Yang, D. Mott, W. Fang, N. Kang, J. Luo, C. Zhong, Langmuir 29 (2013) 9249–9258.
[7] R. Singh, R. Awasthi, Catal. Sci. Technol. 1 (2011) 778–783.
[8] T. Maiyalagan, K. Scott, J. Power Sources 195 (2010) 5246–5251.
[9] Z. Cai, C. Liu, G. Wu, X. Chen, X. Chen, Electrochim. Acta 112 (2013) 756–762.
[10] P. Shen, Z. Yan, H. Meng, M. Wu, G. Cui, R. Wang, L. Wang, K. Si, H. Fu, RSC Adv. 1 (2011) 191–198.
[11] M.M. Ottakam Thotiyl, T. Ravi Kumar, S. Sampath, J. Phys. Chem. C 114 (2010) 17934–17941.
[12] S. Lin, J. Chen, Y. Hsieh, P. Wu, Mater. Lett. 65 (2011) 215–218.
[13] A. Geraldes, D. da Silva, E. Pino, J. da Silva, R. de Souza, P. Hammer, E. Spinacé, A. Neto, M. Linardi, M. dos Santos, Electrochim. Acta 111 (2013) 455–465.
[14] A. Safavi, H. Kazemi, S. Momeni, M. Tohidi, P. Khanipour Mehrin, Int. J. Hydrogen Energy 38 (2013) 3380–3386.
[15] R. Modibedi, T. Masombuka, M. Mathe, Int. J. Hydrogen Energy 36 (2011) 4664–4672.
[16] S. Shen, T. Zhao, Q. Wu, Int. J. Hydrogen Energy 37 (2012) 575–582.
[17] X. Wang, G. Ma, F. Zhu, N. Lin, B. Tang, Z. Zhang, Electrochim. Acta 114 (2013) 500–508.
[18] T. Ramulifho, K. Ozoemena, R. Modibedi, C. Jafta, M. Mathe, Electrochim. Acta 59 (2012) 310–320.
[19] A. Hao, L. Pan, H. Cui, B. Li, D. Zhou, J. Zhai, Q. Li, Electrochim. Acta 102 (2013) 79–87.
[20] D. Chu, J. Wang, S. Wang, L. Zha, J. He, Y. Hou, Y. Yan, H. Lin, Z. Tian, Catal. Commun. 10 (2009) 955–958.
[21] K. Ding, H. Yang, Y. Cao, C. Zheng, S. Rapole, Z. Guo, Mater. Chem. Phys. 142 (2013) 403–411.
[22] Z. Zhang, L. Xin, K. Sun, W. Li, Int. J. Hydrogen Energy 36 (2011) 12686–12697.
[23] R. Li, Z. Wei, T. Huang, A. Yu, Electrochim. Acta 56 (2011) 6860–6865.
[24] Y. Xiao, G. Yu, J. Yuan, J. Wang, Z. Chen, Electrochim. Acta 51 (2006) 4218–4227.
[25] S. Shen, T. Zhao, J. Xu, Y. Li, J. Power Sources 195 (2010) 1001–1006.
[26] K. Lee, S. Kang, S. Lee, K. Park, Y. Lee, S. Han, ACS Appl. Mater. Interfaces 4 (2012) 4208–4214.
[27] H. Wang, Z. Liu, S. Ji, K. Wang, T. Zhou, R. Wang, Electrochim. Acta 108 (2013) 833–840.
[28] Y. Ma, H. Wang, S. Ji, V. Linkov, R. Wang, J. Power Sources 247 (2014) 142–150.
[29] K. Wang, H. Wang, R. Wang, J. Key, V. Linkov, S. Ji, S. Afr. J. Chem. 66 (2013) 86–91.
[30] J. Kang, R. Wang, H. Wang, S. Liao, J. Key, V. Linkov, S. Ji, Materials 6 (2013) 2689–2700.
[31] R. Wang, Z. Zhang, H. Wang, Z. Lei, Electrochem. Commun. 11 (2009) 1089–1091.
[32] J. Silva, L. Parreira, R. De Souza, M. Calegaro, E. Spinacé, A. Neto, M. Santos, Appl. Catal. B 110 (2011) 141–147.
[33] J. Kim, J. Heo, S. Hwang, S. Yoo, J. Jang, J. Ha, S. Jang, T. Lim, S. Nam, S. Kim, Int. J. Hydrogen Energy 36 (2011) 12088–12095.
[34] Y. Wang, F. Shi, Y. Yang, W. Cai, J. Power Sources 243 (2013) 369–373.
[35] T. Ramulifho, K.I. Ozoemena, R.M. Modibedi, C.J. Jafta, M.K. Mathe, Electrochim. Acta 59 (2012) 310–320.
[36] X. Mao, L. Yang, J. Yang, J. Key, S. Ji, H. Wang, R. Wang, J. Electrochem. Soc. 160 (2013) H219–H223.
[37] X. Zhang, H. Wang, J. Key, V. Linkov, S. Ji, X. Wang, Z. Lei, R. Wang, J. Electrochem. Soc. 159 (2012) B270–B276.
[38] T. Bligaard, J. Nørskov, Electrochim. Acta 52 (2007) 5512–5516.
[39] J. Wang, H. Inada, L. Wu, Y. Zhu, Y. Choi, Pi Liu, W. Zhou, R. Adzic, J. Am. Chem. Soc. 131 (2009) 17298–17302.
[40] Y. Feng, Z. Liu, Y. Xu, P. Wang, W. Wang, D. Kong, J. Power Sources 232 (2013) 99–105.